SYNTHESIS AND CHARACTERIZATION OF CHEMICAL BATH DEPOSITED COPPER DOPED LEAD SULFIDE THIN FILMS

Dennis Eyetan Elete[1], Joseph Onyeka Emegha[2*], Nelson Oyindenyifa Nenuwe[1] and Oghogho Weyinmi Omagbemi[1]

[1]Department of Physics, Federal University of Petroleum Resources, Effurun, Delta State, Nigeria

[2]College of Natural and Applied Sciences, Novena University Ogume, Kwale, Delta State, Nigeria

ABSTRACT. The effects of copper concentration on the properties of copper lead sulfide ($Cu_xPb_{1-x}S$) thin films have been reported. Chemical bath deposition (CBD) method was used to deposit the ternary material on soda-lime substrates. Here, the $Cu_xPb_{1-x}S$ films were grown using copper(II) chloride, lead nitrate, and thiourea as sources of copper (Cu), lead (Pb) and sulfur (S), respectively. The grown films were examined using X-ray diffractometer (XRD), scanning electron microscopy (SEM), energy dispersive X-ray (EDX) spectroscopy, UV-spectrophotometer and four-point (4P) probes. XRD measurements revealed a polycrystalline material with strong adherent to the substrates. SEM readings indicated various grain-like crystalline morphologies with different sizes that change with copper concentrations. The EDX studies revealed that the deposited material consist of copper, lead and sulfur in various compositions. The transmittance was high in the near infrared regions of the electromagnetic radiation and, also decreases with copper concentrations. The band gap (E_g) varies from 2.05 to 2.50 eV with increase in copper concentrations. The study shows that CBD is an excellent method in depositing good quality films for device applications.

KEY WORDS: Thin films, Substrates, Copper lead sulfide, Deposition, Optical properties

INTRODUCTION

Lead sulfide (PbS) is an importance semiconducting material that belongs to group IV-VI of the periodic table [1, 2]. It possesses excellent optoelectronic properties and finds applications in light emitting diodes, photovoltaic cells, cathode-luminescence and electroluminescent displays, optical switch multilayer dielectric filters, sensor, lasers and catalysis [1]. At room temperature, PbS possesses narrow band gaps of about 0.4–1.35 eV in the UV region [3, 4]. It can virtually be deposited with all chemical and physical methods. Lead sulfide appears as a black coloured crystal or powder with a density of 7.60 gcm^{-3} and molecular mass of 239.30 $gmol^{-1}$. It crystallizes in halite (cubic) structures with the (lattice) constant a = 5.936 Å [5]. Recently, investigation into new photovoltaic materials with improved efficiency have assumed a considerable interest and researchers are investigating to understand the characteristics of PbS films for opto-electronic applications [6]. Doping with elements like copper has shown to enhance the structural, optical and electrical properties of PbS thin films.

Copper doped lead sulfide ($Cu_xPb_{1-x}S$) thin films have attracted a great deal of attention due to its applications. Usually, wide ranges of solubility of lead and copper ions in ternary copper lead sulfide compound can be expected, as these ions can fill either substitutional or interstitial positions of the resulting films [7]. The structure of copper lead sulfide thin film may not be unstoichiometric, as the vacancies control the conductivity type which may causes variations in conductivity [8]. These properties of ternary copper doped lead sulphide thin films have attracted great interest in the fundamental studies on the films. These properties depend on the preparation methods as well as parameters like substrates, impurity level and post-deposition processing [1].

_____

Thin films of miscible systems have been grown utilizing different deposition techniques and these techniques have their different deficiencies [9]. The application of CBD technique has received much attraction due to its great potential to fabricate high quality films [2, 10]. It is a preparative method well-suited for large scale production which is cost effective comparing with other deposition methods [10]. The method was used in the past to synthesize crystalline and polycrystalline binary sulfides and oxides [11]. Recently, CBD technique is desired to synthesize ternary and quarternary materials for device applications.

Reports on the fabrication and characterization of various binary copper-sulfide and lead-sulfide thin films using different deposition techniques are relatively common in the literature [1-3], but work on their ternary compound of copper lead sulfide ($Cu_xPb_{1-x}S$) is less common. In this work, we investigate the effect of copper concentrations on the properties of $Cu_xPb_{1-x}S$ thin films using the chemical bath deposition (CBD) technique. The interest in ternary materials comes from the possibility of engineering the elemental parameters with deposition. Then again, ternary compounds are attracting increasing attention due to their good performances with moderately simple chemistry and the absence of environmental concerns associated with their uses. This research presents the synthesis of the ternary $Cu_xPb_{1-x}S$ thin films via the CBD technique. In addition, the effects of copper concentrations on the properties of $Cu_xPb_{1-x}S$ thin films, which, hitherto has not been studied were examined.

EXPERIMENTAL

Materials

To synthesis $Cu_xPb_{1-x}S$ thin films, chemicals (analytical grade) were used without further purification; The chemicals employed for the films preparation, along with their sources and percentage purity are listed as follows; lead nitrate, $Pb(NO_3)_2$ (BDH, purity = 99.0%), copper(II) chloride, $CuCl_2.2H_2O$ (Assay = 99.0%), thiourea, $NH_2.CS.NH_2$ (LABOSI, purity = 98.0%), EDTA disodium salt (Arochem Pvt. purity = 98.0%), ammonia solution, NH_4OH (Alfa India, 25%) and distilled water.

Deposition of $Cu_xPb_{1-x}S$ thin films

Solutions of 1.0 M of copper(II) chloride, lead nitrate and thiourea were prepared from accurately weighed analytical solids. 25 mL of each solution was taken into a separate beaker to form 75 mL of the solution. Then 25 mL of distilled water was used to top the solution to 100 mL. It was then stirred for about 30 min for proper harmonization of the ions. During the deposition, EDTA disodium salt was used as a complexing agent. 25% of ammonia solution was added drop-wise using a burette to maintain the pH of the solution at 9.0. Constant volumes of lead nitrate, thiourea, ammonia solution and the EDTA disodium was maintained. When doping with copper, varying volumes of uniform concentration of $CuCl_2.2H_2O$ solutions was used by changing the concentration of x in $Cu_xPb_{1-x}S$ nanostructured thin films;

$$x = \frac{[Cu^{2+}]}{[Pb^{2+} + Cu^{2+}]} \qquad (1)$$

where, Cu^{2+} and Pb^{2+} are the number of moles of copper(II) chloride and lead nitrate respectively. However, the value of x varied from 0.0 to 0.4 using the relation $Cu_xPb_{1-x}S$. Table 1 indicates how the deposition conditions were varied.

Table 1. Parameters of depositing $Cu_xPb_{1-x}S$ thin films.

Sample	Molecular precursors concentrations and volume
A	$CuCl_2.2H_2O$ (1.0 M, 0 mL) + $Pb(NO_3)_2$ (1.0 M, 10 mL) + $NH_2.CS.NH_2$ (1.0 M, 20 mL)
B	$CuCl_2.2H_2O$ (1.0 M, 0.2 mL) + $Pb(NO_3)_2$ (1.0 M, 0.8 mL) + $NH_2.CS.NH_2$ (1.0 M, 20 mL)
C	$CuCl_2.2H_2O$ (1.0 M, 0.3 mL + $Pb(NO_3)_2$ (1.0 M, 0.7 mL) + $NH_2.CS.NH_2$ (1.0 M, 20 mL)
D	$CuCl_2.2H_2O$ (1.0 M, 0.4 mL) + $Pb(NO_3)_2$ (1.0 M, 0.6 mL) + $NH_2.CS.NH_2$ (1.0 M, 20 mL)

Characterization techniques

The crystalline characterization was measured using D8 High Resolution X-ray diffractometer with wavelength of λ = 1.5406 Å. Morphological and elemental compositions were observed by JEOL JSM-7600F Scanning electron microscopy (SEM). Optical measurements were done through a (UV-1800S) Spectrophotometer in a wavelength range of 350 to 800 nm at room temperature, while four-point probes were used to determine the electrical properties.

RESULTS AND DISCUSSION

X-ray crystallization

The crystallization patterns of the films are illustrated in Figure 1. The pattern of sample A (PbS) is illustrated in Figure 1(a). The spectrum shows diffraction peaks 2θ at 28.0^o, 30.3^o, 33.0^o, 35.01^o and 51.03^o corresponding to diffraction lines of (111), (222), (200), (400) and (440) plane from the face centre cubic phase of lead sulfide (card number 0078-1901). The presence of several sharp peaks confirms the polycrystalline character of the deposited PbS thin films. It is also observed that there is one preferred growth orientation of (222) plane, with intensity that is reliant on the preparation parameters. Moreover, the absence of any other peaks shows that the material is free of impurities. Figure 1(b) shows the pattern of sample B ($Cu_{0.2}Pb_{0.8}S$). The sharp peaks were seen at approximately 2θ = 28.0^o, 30.3^o, 33.0^o, 35.01^o and 51.03^o. These intense peaks confirm the polycrystalline nature of the deposited material. Illustrated in Figure 1(c), is the pattern of sample C ($Cu_{0.3}Pb_{0.7}S$). The presence of peaks, also, indicated a polycrystalline film. The peaks appeared at diffraction angle of 2θ = 28.0^o, 30.3^o, 33.0^o, 35.01^o and 51.03^o. Figure 1(d) showed the pattern of sample D ($Cu_{0.4}Pb_{0.6}S$). Peaks appeared at 28.0^o, 30.3^o, 33.0^o, 35.01^o and 51.03^o planes, matching the (111), (222), (200), (400) and (440) planes. The peaks matched well with the standard copper-lead-sulfide diffraction peaks.

From the analysis of $Cu_xPb_{1-x}S$ thin films, it showed that the intensities of the peak at 2θ = 30.3^o increases with copper concentrations. This increase in peak intensity may result from the induced structural disorder within the deposited films as a result of copper impurities in $Cu_xPb_{1-x}S$ system [12]. The occurrence of well-defined and sharp peaks confirms the polycrystalline nature of the deposited films [13, 14]. Polycrystalline thin films orientations are generally determined by the processing parameters. The changes evident in the structure occur due to surface diffusion as well as grain boundaries migration of two smaller nuclei of different orientation to form a larger one [10].

The crystalline size (D) of the films was calculated from the X-ray diffraction (222) reflection using the Debye- Scherer's relation (2) [15]

$$D = \frac{k\lambda}{\beta \cos\theta} \tag{2}$$

where β is the measured FWHM (in radiant), θ is the Bragg angel of the peak, the λ is the X-ray diffraction wavelength, D is the effective crystalline size. The calculated D was 21.144, 22.788, 23.266 and 26.084 nm for the various samples. This shows that the D varies with concentration

but the enlargement was more evident when the concentration was increased from $Cu_{0.3}Pb_{0.7}S$ to $Cu_{0.4}Pb_{0.6}S$.

Morphological study

The variations in surface morphology at different doping concentrations are illustrated in Figure 2. As indicated, the substrates were well covered with films of different morphological structures. For Sample A (PbS), the SEM micrograph shows cloudy images, which confirms a polycrystalline grains formation within the films. It was also, seen, that copper concentration highly influences the surface morphologies of the samples, as Sample B shows rougher films with the creation of some compact grain-like features. Evidently, the gradual formation of grain-like features was due to the increase nucleation rate as the doping concentration is increased. Further increase in doping concentrations (Samples C and D), increased the creation of more grains. Therefore, maintaining the non-uniform and close-packed morphology over the substrate. Moreover, the increased formations of black and white grains were also observed, which originated from the variation of lead and copper content within the $Cu_xPb_{1-x}S$ matrix. This may explain the coexistence of lead and copper in the $Cu_xPb_{1-x}S$ system as indicated from the x-ray diffractometry (XRD) measurement. The larger grains were found to detach into smaller and well-organized quasi-spherical polycrystalline grains (Sample D). This development parallel the fact that increasing the deposition concentration results in a number of grains diffusing and coalescing simultaneously to form sizable crystalline grains with defined crystallographic morphologies as revealed from the scanning electrode microscopy (SEM) studies[15]. Furthermore, the different morphological structures exhibited by this material may be the direct results of the various phases and elemental compositions of the material suggested from the XRD studies.
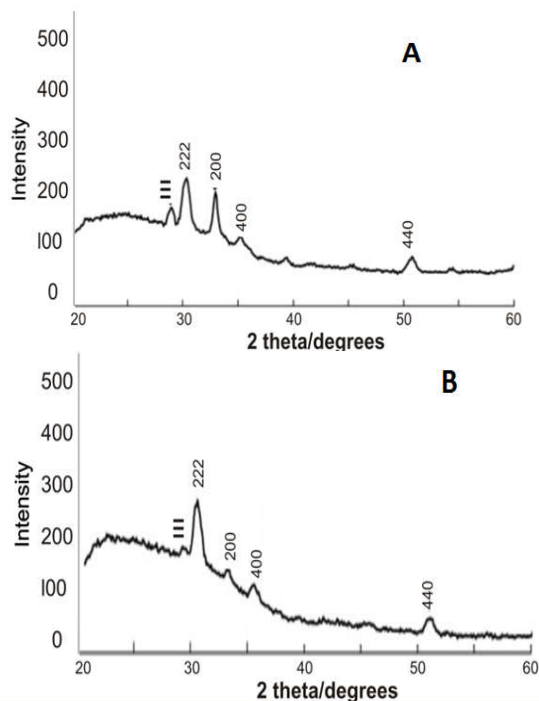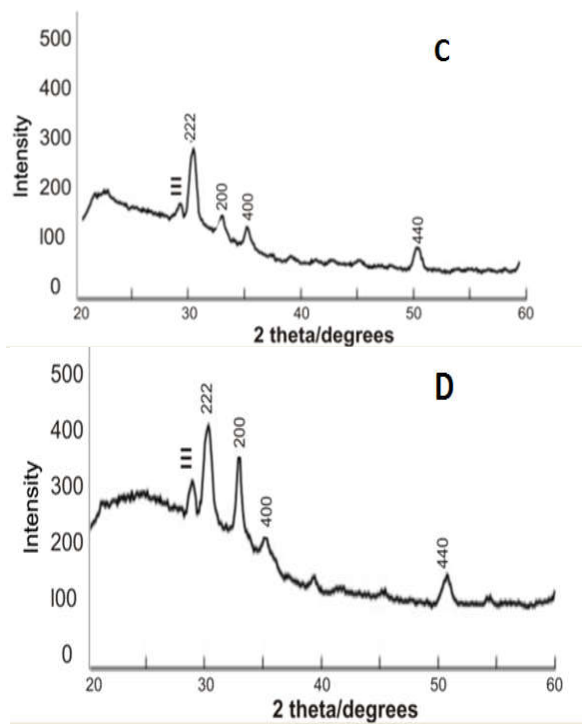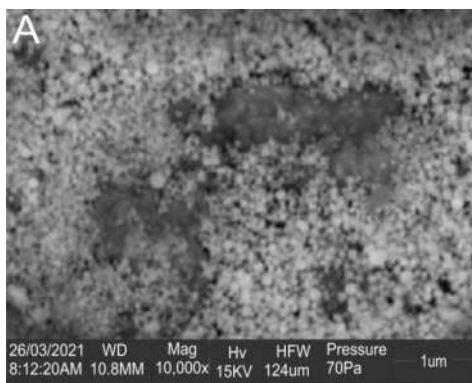
Figure 1. XRD spectrum for (A) PbS (B) $Cu_{0.2}Pb_{0.8}S$ (C) $Cu_{0.3}Pb_{0.7}S$ (D) $Cu_{0.4}Pb_{0.6}S$.
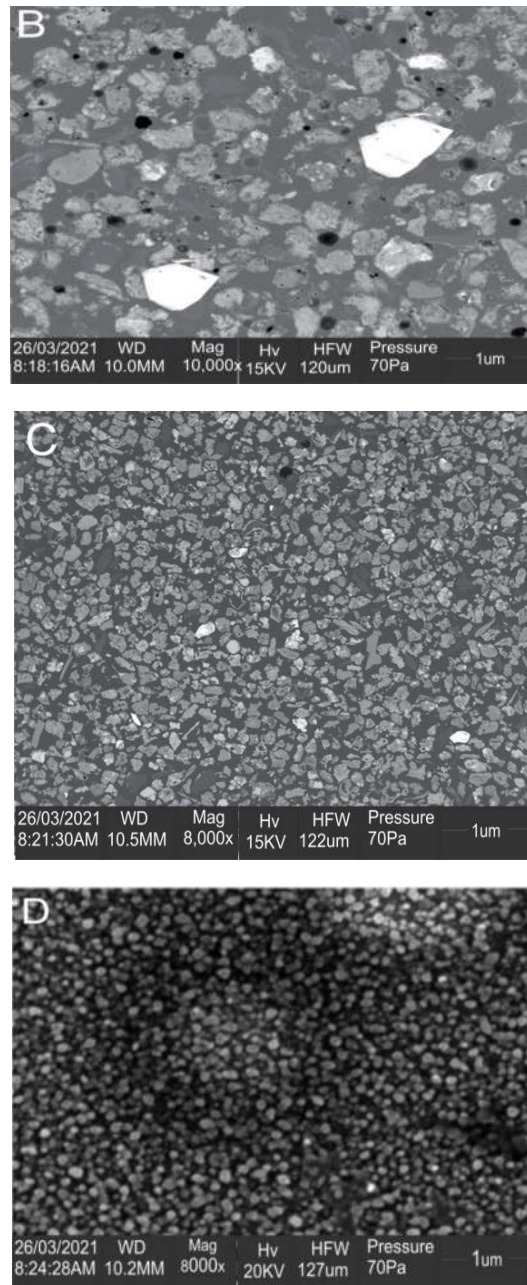
Figure 2. The SEM image for (A) PbS (B) $Cu_{0.2}Pb_{0.8}S$ (C) $Cu_{0.3}Pb_{0.7}S$ (D) $Cu_{0.4}Pb_{0.6}S$.

Elemental analysis

The elemental analysis of the undoped lead sulphide (PbS) thin films demonstrate that the lead (Pb) atomic percentage is 20.34 and that of sulfur (S) is 49.40 as indicated in Figure 3(a). The S/(Cu + Pb) atomic ratio is 2.43 as shown in Table 2, which indicates that the sulfur atoms are in excess and could occupy either the interstitial sites or at the regular sites by creating equivalent number of lead (Pb) vacancies. Also indicated in the energy dispersive X-ray (EDX) spectrum in Figure 3(a), is the large amount of oxygen within the deposited film. This large amount of oxygen may be attributed to the abundance of oxygen in the starting material as well as the migration of these elements (oxygen) from the glass slide to the films during deposition [15]. Figures 3 (b-d) illustrate the EDX spectrums of copper doped lead sulfide thin films. When the intrinsic lead sulfide (PbS) is doped with Cu ions, the copper ions will successfully occupy the Pb^{2+} sites, thus reducing the S/(Cu + Pb) ratio below 1.0, as indicated in Table 2. This means that more copper atoms can diffuse into the PbS lattice without altering the host crystal structure as indicated from the X-ray diffractometry (XRD) measurements. The EDX measurements also showed that the elemental compositions of the doped material consist of copper (Cu), lead (Pb) and sulfur (S), which imply that the $Cu_xPb_{1-x}S$ film is non-stoichiometric. It is reasonable to assume that the increase in copper concentration raises the rate of nucleation of atoms in the precursor and, after that, the elements in the $Cu_xPb_{1-x}S$ system.

Table 2. Summary of the EDX analysis of $Cu_xPb_{1-x}S$ films.

Samples	Elemental composition (%)			S/(Cu + Pb)	E_g	n
	Cu	Pb	S			
A	-	20.34	49.40	2.43	2.05	1.8
B	45.25	48.20	6.20	0.07	2.10	1.8
C	50.26	30.45	9.40	0.12	2.20	2.0
D	40.04	12.30	47.66	0.91	2.50	1.6
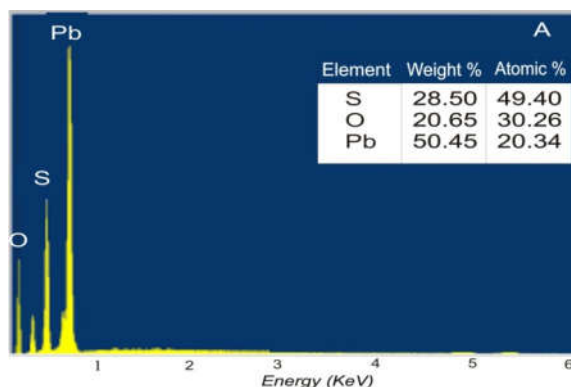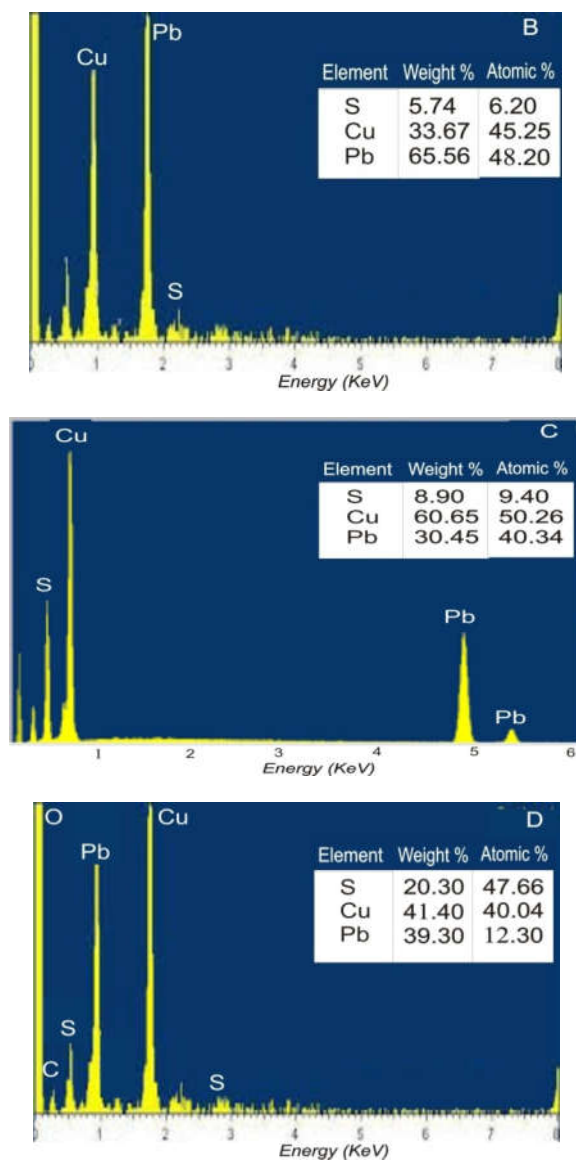
Figure 3. EDX spectrum for sample (A) PbS, (B), $Cu_{0.2}Pb_{0.8}S$, (C) $Cu_{0.3}Pb_{0.7}S$, (D) $Cu_{0.4}Pb_{0.6}S$.

Optical analysis

The transmittance spectra and wavelength plot is shown in Figure 4. It was found that the films had a very high transmittance of above 75% in the visible and near infrared regions. Sample C had the least transmittance in the infrared region while sample D had the highest in same region. Also, copper concentrations were decreasing with transmittance, except for sample D. This

decrease may result from the formation of copper doped lead sulfide nanocrystals, which are increasing with transparency [16]. Therefore, reduction of copper concentrations makes the films more transparent. The high transmittance observed was due to the improved crystallinity of the films, which in turn, reduces the defects in the grains. Films of such high transmittance could be used for several applications, including solar cells, transparent conducting materials in light emitting diodes (LEDs) and photonic devices [17, 18]. The optical absorbance against wavelength is indicated in Figure 5. It was observed that the absorption was high in the ultraviolet region of the spectra. Also, from the spectra, the absorbance increases with increasing copper concentrations. An indication of an improve transmission and crystallinity within the films [19]. Generally, the absorbance values were seen to be low throughout the visible and near infrared regions and range between 0.02 and 0.12. The refractive index (n) against photon energy is indicated in Figure 6. From the graph, the refractive indexes were decreasing with photon energy. The highest refractive index was established to be approximately 2.02 in the high energy region. However, as the doping concentration is increased, the average refractive indexes fall, and rise within the values of 1.57 and 2.02 (Table 2). This trend in 'n' was possibly due to the trapped photon energy within the deposited thin films [13, 16].

The direct band gap (E_g) of the films was estimated by plotting $(\propto h\nu)^2$ against photon energy ($h\nu$). Figure 7(a-d) shows the plot of various samples. For all compositions, the E_g increases with copper concentration as depicted in Table 2. The variation in E_g with copper concentration was seen to be somewhat linear which is due to the E_g of copper sulfide (CuS) being greater than that of lead sulfide (PbS) thin films (Table 2). This increase toward higher energy side is in accordance with the trend reported in literature for ternary materials with two binary constituents [10]. The increase in E_g shows an improvement in structural crystallinity or phase transformation taking place within the films as a result of increased copper concentrations, as indicated in the XRD and SEM measurements [20]. Also, it could be due to the famous Burstein-Moss effect [21]. When copper atoms are deeply doped into lead sulfide (PbS) thin films, the lower levels in the conduction bands are occupied by electrons resulting in an increased Fermi level and then the E_g as well [22]. Another possibility for the E_g increase could be credited to the existence of secondary phases in small quantity that may not be detected within the films [23].
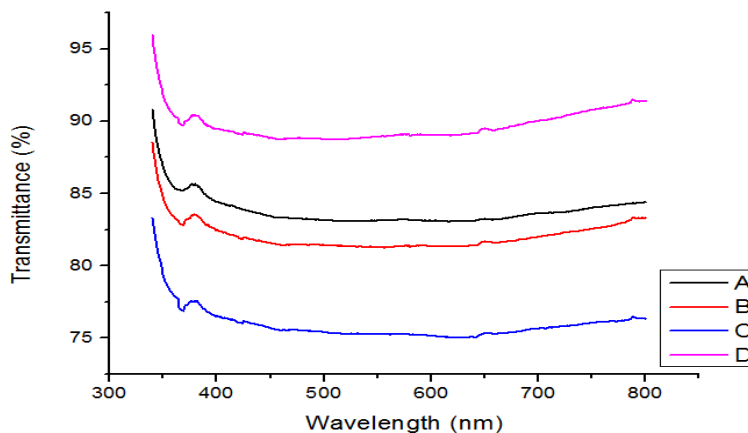

Figure 4. Transmittance spectrum for (A) PbS, (B) $Cu_{0.2}Pb_{0.8}S$, (C) $Cu_{0.3}Pb_{0.7}S$ and (D) $Cu_{0.4}Pb_{0.6}S$.
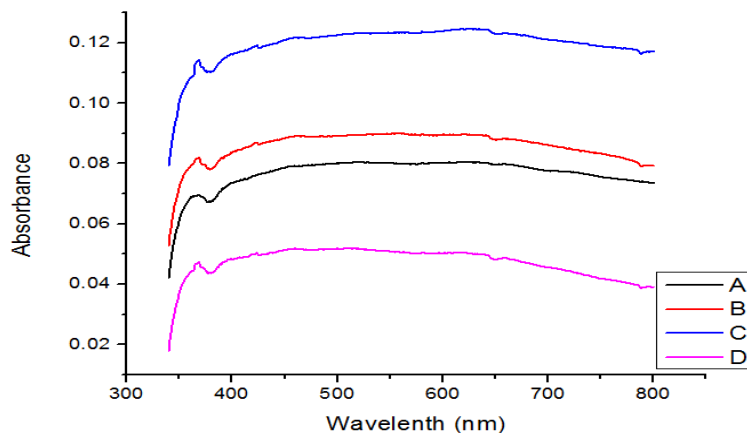
Figure 5. Absorbance Spectrum for (A) PbS (B) $Cu_{0.2}Pb_{0.8}S$ (C) $Cu_{0.3}Pb_{0.7}S$ (D) $Cu_{0.4}Pb_{0.6}S$.
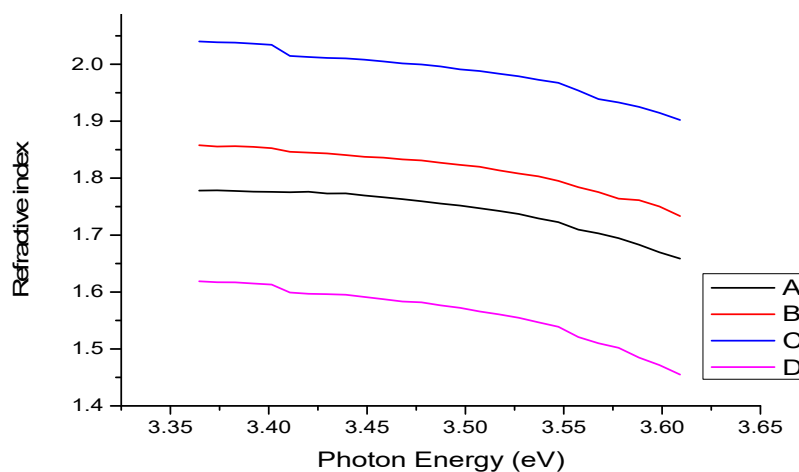
Figure 6. Refractive Index of (A) PbS (B) $Cu_{0.2}Pb_{0.8}S$ (C) $Cu_{0.3}Pb_{0.7}S$ (D) $Cu_{0.4}Pb_{0.6}S$.

Electrical (I-V) characterization of the thin films

The I-V study was done using the four-point probe technique. The sheet resistivity and conductivity of $Cu_xPb_{1-x}S$ thin films were measured and the results were indicated in Figure 8. From Figure 8, the electrical resistivity at very low concentration was valued at 10^3 Ωcm and then increases to the order of 10^5 Ωcm. The resistivity were also increasing with copper concentration which shows that copper doping influences the electrical conductivity of $Cu_xPb_{1-x}S$ thin films. However, as x increases beyond 0.2 (Sample B), the resistivity begins to increase. This may be credited to the nature of the films deteriorating with further increase in the dopant concentration [15]. The nature of the observed conductivity is owed to the improved concentration of the charge carriers within the films system [24]. This reflects the expansion and pairing of grains to form larger crystallites within the $Cu_xPb_{1-x}S$ system.
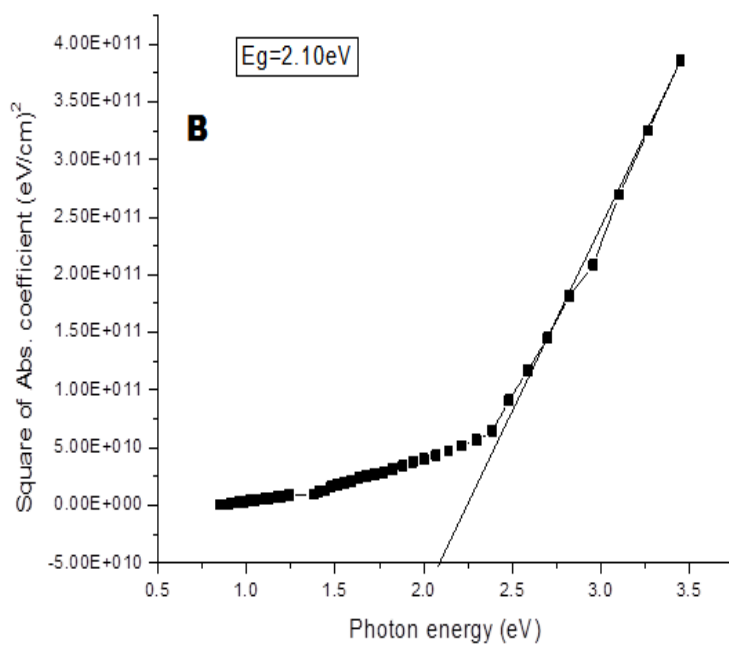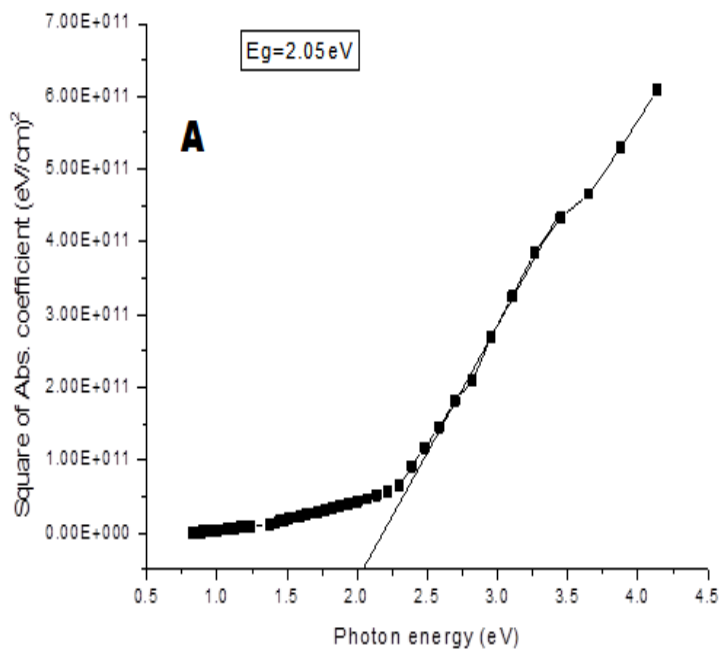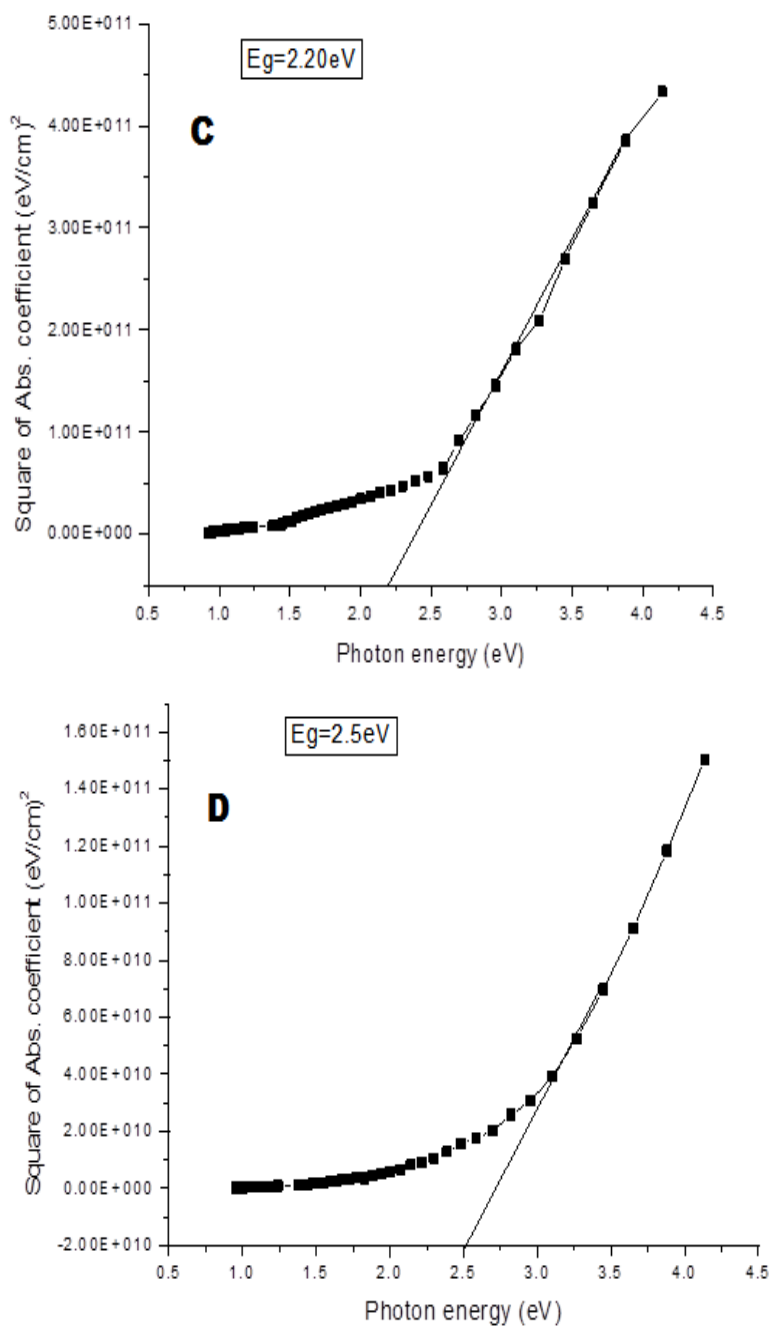
Figure 7. Square of absorption coefficient versus photon energy for Sample (A) (PbS), (B) $(Cu_{0.2}Pb_{0.8}S)$, (C) $Cu_{0.3}Pb_{0.7}S$ and (D) $(Cu_{0.4}Pb_{0.6}S)$.
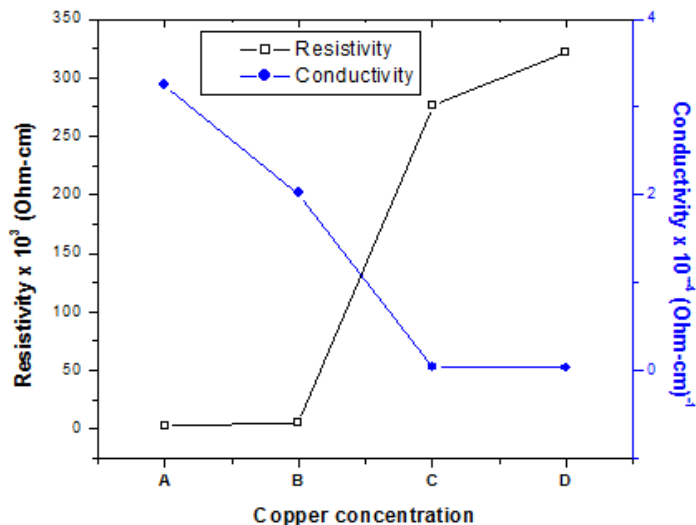
Figure 8. Conductivity and resistivity of $Cu_xPb_{1-x}S$ thin films.

CONCLUSION

Ternary copper doped lead sulfide ($Cu_xPb_{1-x}S$) thin films were achieved through the CBD techniques. The route offers a unique technique in preparing copper doped lead sulfide thin films utilizing common bath solutions. Structural, elemental, morphological, optical as well as the I-V characteristics were directly influenced by the dopant concentrations. The EDX measurement corroborated that the films comprise of copper (Cu), lead (Pb) and sulfur (S) in various elemental compositions. SEM revealed an agglomeration of grains with different morphological forms. The films show high transmittance of above 75% in the UV region with an energy gap that increased from 2.05 to 2.50 eV with copper concentrations. Thus, confirming the suitability of $Cu_xPb_{1-x}S$ thin films for various device applications. Since, a surface-sensitive quantitative spectroscopic method based on the photoelectric effect called X-ray photoelectron spectroscopy (XPS) can identify the elements present in a material (its elemental composition) or that are present on its surface, as well as their chemical state, general electronic structure, and density of the electronic states in the material. It is therefore suggested that future studies be conducted on XPS data (which will reveal the oxidation states of elements) as well as XPS depth profiling. Also, the Hall Effect measurements were not considered during this study due to limitations in the device used for the study. However, these will be considered in future scope so as to determine the types of carrier concentrations, mobility of the carriers as well as the hall coefficients of the material wherein the four point probes cannot provide such a feature.

REFERENCES

1. Omotoso, E.; Adegboyega, G.A.; Eleruja, M.A.; Olofinjana, B.; Akinwunmi, O.O.; Ilori, O.O.; Taleatu, B.A.; Ajayi, E.O.B. Synthesis and some properties of MOCVD lead sulphide and lead sulphide thin films. *J. Non oxide Glasses* **2013**, 5, 9-19.

2. Abbas, M.M.; Shehab, A.A.; Al-Samuraee, A.K.; Hassan, N.A. Effect of deposition time on the optical characteristics of chemically deposited nanostructured PbS thin films. *Energy Procedia.* **2011**, 6, 241-250.

3. Min, S.H. Chemical bath deposited lead sulphide thin films: preparation and characterization, *World J. Mech.* **2014**, 1, 1-6.

4. Orori, M.C. *Electrical and optical characterization of $Cd_xZn_{1-x}S$ and PbS thin films for photovoltaic applications.* MSc Thesis, Kenyetta University, Nairobi, Kenya, **2012**.

5. Fekadu, G.H. *Synthesis and characterization of cadmium selenide (CdSe) and lead sulphur selenide ($PbS_{1-x}Se_x$) thin films by chemical bath deposition method.* PhD Thesis, Kwame Nkrumah University of Science and Technology. Kumasi, Ghana, **2015**.

6. Tariq, G.H.; Hutchings, K.; Asghar, G.; Lane, D.W. Study of annealing effects on the physical properties of evaporated SnS thin films for photovoltaic application. *J. Ovonic Res.* **2014**, 6, 247-256.

7. Santos-Cruz, J.; Coronel-Hernandez, J.; Mayen-Harnandez, S.A.; Santos-Cruz, D.; Moure-Flores, F.; Perez-Garcia, S.A.; Licea-Jimenez, L.; Arenas-Arrocena, M. Optical, electrical and photocatalytic properties of the ternary semiconductors $Zn_xCd_{1-x}S$, $Cu_xCd_{1-x}S$ and $Cu_xZn_{1-x}S$. *Int. J. Photoenergy* **2014**, 158782, 1-8.

8. Emegha, J.O.; Damisa, J.; Efe, F.O.; Olofinjana, B.; Eleruja, M.A.; Azi, S.O. Preparation and characterization of metal organic chemical vapour deposited copper zinc sulphide thin films using single solid source precursors. *Eur. J. Mater. Sci. Eng.* **2019**, 4, 11-22.

9. Uhuegbu, C.C. *Growth and characterization of ternary chalcogenide thin films for efficient solar cells and possible industrial applications.* Ph.D. Thesis, Covenant University, Nigeria, **2007**.

10. Emegha, J.O.; Damisa, J.; Elete, D.E.; Arijaje, T.E.; Akinpelu, A.; Ogundile, P.O.; Onumejor, C.A. Growth and characterization of copper cadmium sulphide thin films. *J. Phys.: Conf. Ser.* **2021**, (1734), 012045.

11. Khatri, R.P.; Patel, A.J. A comprehensive review on chemical bath deposited ZnS thin films. *IJRASET.* **2018**, 6, 1705-1722.

12. Adeoye, A.E.; Ajenifuja, E.; Taleatu, B.A.; Fasasi, A.Y. Rutherford backscattering spectrometry analysis and structural properties of $Zn_xPbn_{1-x}S$ thin films deposited by chemical spray pyrolysis. *J. Mater.* **2015**, 2015, Article ID 215210.

13. Damisa, J.; Emegha, J.O. XRD and UV-Vis spectroscopic studies of lead tin sulphide (PbSnS) thin films. *Trends Sci.* **2021**, 18, 16.

14. Damisa, J.; Emegha, J.O.; Ikhioya, I. L. Deposition Time induced Structural and Optical Properties of Lead Tin Sulphide Thin Films. *J. Nig. Soc. Phys. Sci.* **2021**, 3, 455–458.

15. Emegha, J.O.; Ukhurebor, K.E.; Aigbe, U.O.; Olofinjana, B.; Azi, S.O.; Eleruja, M.A. Effect of deposition temperature on the properties of copper-zinc sulphide thin films using mixed copper and zinc dithiocarbamate precursors. *GU. J. Sci.* **2022**, 35, 1556-1590.

16. Emegha, J.O.; Elete, E.D.; Efe, F.O.; Adebisi, A.C. Optical and electrical properties of semiconducting ZnS thin films prepared by chemical bath deposition. *JMSRR.* **2019**, 4, 1-8.

17. Olofinjana, B.; Egharevba, G.O.; Taleatu, B.A.; Akinwunmi, O.O.; Ajayi, E.O.B. Effect of deposition temperature on some properties of MOCVD molybdenum sulphide thin films. *J. Mater. Sci. Eng.* **2014**, 4, 78-82.

18. Usoh, C.I.; Okujagu, C.U. Spectral analysis of amorphous thin films of MnS obtained chemically by varying solution concentrations. *Res. J. Phys. Sci.* **2014**, 2, 1-8.

19. Mereh, A.U.; Momoh, M.; Hamza, B. Influence of substrate temperature on optical properties of nanostructured $CuAlb_2$ thin films grown by two stage vacuum thermal evaporation technique. *Int. J. Eng. Sci. Invention.* **2013**, 2, 48-52.

20. Ziaer, A.; Meftah, A.; Jaber, A.Y.; Abdelaziz, A.A.; Aida, M.S. Annealing effects on the structural electrical and optical properties of ZnO thin films prepared by thermal evaporation technique. *J. King Saud Univ. Sci.* **2015**, 27, 356-360.

21. Choge, C.H. *Optical and electrical characterization of ZnSe-CU$_x$O$_Y$ thin films for solar cell applications*. MSc Thesis. Kenyatta University, Nairobi, Kenya, **2016**

22. Zhang, H.; Shugang, Y.; Hanfa, L.; Changkun, Y. Preparation and characterization of transparent conducting ZnO:W films by dc magnetron sputtering. *J. Semicond*. **2011**, 32, 430021 - 430024.

23. Nagamani, K.; Reddy, M.V.; Lingappa, Y.; Ramakrishna Reddy, K.T.; Miles, R.W. Physical properties of Zn$_x$Cd$_{1-x}$S nanocrystallite layers synthesized by solution growth method. *Int. J Optoelectronic Eng*. **2012**, 2, 1-4.

24. Emegha, J.O.; Olofinjana, B.; Ukhurebor, K.E.; Adegbite, J.T.; Eleruja, M.A. Electrical properties of semiconducting copper zinc sulphide thin films. *Curr. Appl. Sci. Technol.* **2022**, 22, 1-9.